intervals are involved. This, unfortunately, is a function of the method of measurement, where the error is a function of full scale deflection.

5.1.3 DISCUSSION OF RESULTS

The theoretical and experimental flow/pressure drop results shown in Figure 5.1 indicate that the flow discharge coefficients are not modified by the onset of cavitation, as shown by the lack of divergence from the linear equation fitted to the data, i.e. the flow rate remains proportional to the 0.5 power of the pressure drop across the orifice during cavitation. This result is supported by the discussion by Ball J.W. on the paper by Numachi F. et al (1960) and by the results given by Ball J.W. et al (1975) which show no modification to the discharge coefficient during cavitation. This result can be explained by the positioning of the upstream and downstream pressure taps. The differential pressure measurement used was made between positions where the pressure measurements were least sensitive to the relative position of the orifice and hence it would seem to the presence of cavitation. Within the region in which the downstream pressure tap and orifice are located, cavitation commences and terminates. The effect of the two-phase flow is to increase the jet velocity immediately downstream of the orifice (due to reduction of average density).

The accuracy of the flow velocity measurements and the cavitation index are given in Section 5.1.2. The deviation of the experimental flow measurements from the theoretical ones appearing to be greater at high flow rates. This tends to indicate that the method and/or the technique used for flow measurement was not as reliable as originally thought. Possibly the main contributing factor is the switching of the water leaving the test rig, and the simultaneous control of the stop watch. With regard to the cavitation index error, the error is associated with the pressure drop term. However, neither error can account for the differences between experimental and predicted results. This tends to focus more attention on the definition used for incipient cavitation.

In some instances with low pressure or low differential pressures the calculated errors are excessive. In such cases it is realised that considerable error is involved, and that errors increase with particular measurement trends, e.g. the velocity increase or differential pressure decrease.

The measured incipient cavitation limits for the orifices tested differ from those predicted from the work of Ball J.W. et al (1975), as given in Table 5.3 above. This may possibly be due to a relatively poor definition of the incipient cavitation point. However, the photographs indicate the nature of the cavitation to be similar for the selected points, thus indicating a need for cavitation limits to be better defined. Another possible reason, or contributing factor, for the deviation may be that the water used in the test rig had been passed through a centrifugal pump, with a resulting disturbance to the water. This could have created microscopic bubbles which may have served as cavitation sites (Section 2.1.2), the mode of bubble formation in the pump being similar to that of the bubbles which outline the tip vortices shed by propellors, with the rate of bubble generation being dependent on the churning action of the impeller (or the flowrate). Allied to this is the system pressure which could have modified the cavitation resistance of the water (Section 2.2.2.).

In the work of Ball J.W. et al (1975) the water had been drawn from a large reservoir (at an elevation of 70 m) through 915 mm and 660 mm pipes to the test rig. Thus, disturbances to the water would have been minimal, and the main influence on cavitation in their tests would appear to be that of pressure.

The photographs in Figures 5.4 to 5.7 show the progression from no cavitation to cavitation for the d/D = 0.43 orifice. As there was no pressure control valve between the pump and the orifice the pressure upstream of the orifice dropped marginally as the flow rate increased, the main purpose of the photographs being to show the progression of cavitation with increasing flow. In Figure 5.4 the photographs show non-cavitating flow and a condition similar to the onset of cavitation; here, the cavitation bubbles are visible at the outer layer of the jet as it leaves the orifice. The further downstream the bubbles pass, the more dispersed within the flow do the bubbles become, some bubbles appearing to have found their way to the recirculation zone. This indicates that the source of growth of the cavitation bubbles is the orifice. The water which undergoes the greatest change in velocity is that which is initially furthest from the orifice (i.e. at the pipe wall). At the orifice this water forms the outer layer of the jet. From Section 3.1 the greatest turbulence is in the outer layer of the jet leaving the orifice; and from Section 2.1.3, cavitation bubbles are most likely to be formed in a highly turbulent flow. At even higher flow rates (or pressure drops) the level of turbulence increases and it is expected that a greater number of cavitation bubbles will be produced. This effect is clearly demonstrated in the photographs (Figures 5.4 to 5.7 and 5.8 to 5.10).

In Figure 5.5 the cavitation level has increased, and both the jet and the recirculation zone are visible. At the point where the jet has fully expanded and contacted the pipe wall, all that is visible is the white appearance of the bubbles/water mixture. Beyond this point the remaining bubbles that have not collapsed gradually become re-absorbed. This shows that not all of the bubbles produced in a cavitating flow collapse rapidly, thus not all cavitation bubbles have the potential to cause damage to solid boundaries. This result is similar to that discussed in Section 2.3. In the region of bubble re-absorption, the flow had an aerated appearance.

At even higher flow rates (Figure 5.6) the jet and recirculation zone are still mutually distinguishable.

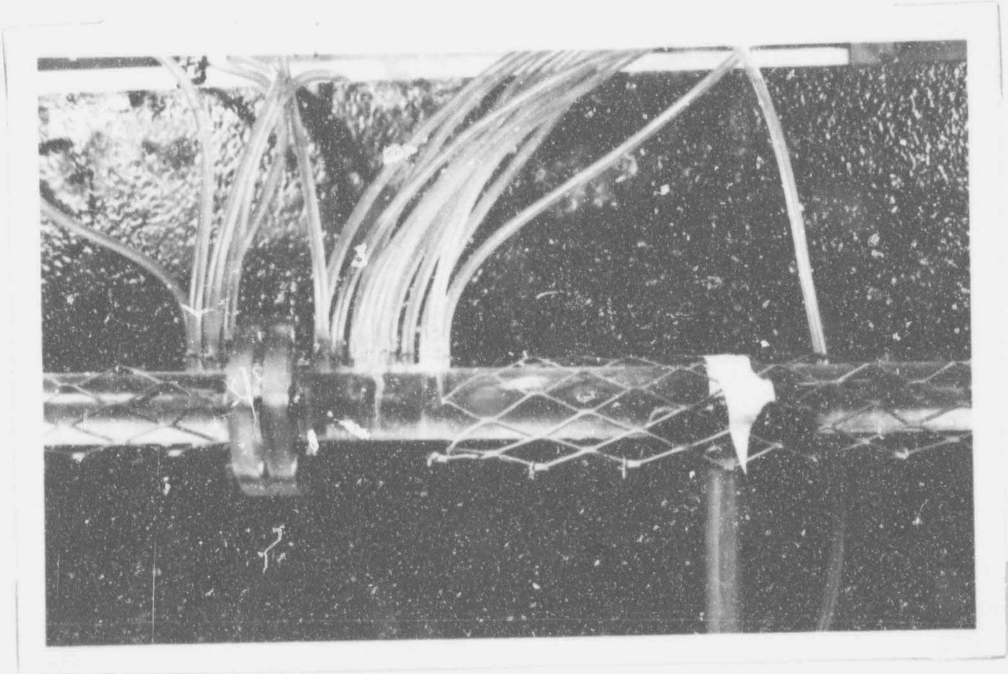

PHOTOGRAPH 1

P_U = 350 kPa ΔP = 178 kPa

Q = 2,11 l/s σ_1 = 1,44

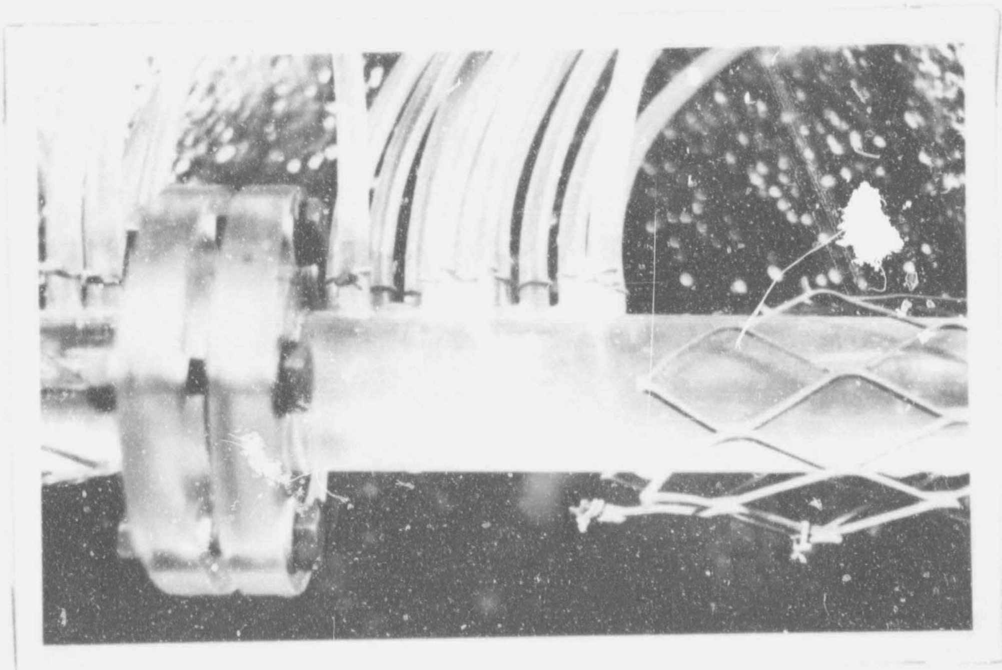

PHOTOGRAPH 2

P_U = 340 kPa ΔP = 274 kPa

Q = 2,6 l/s σ_1 = 0,54

FIGURE 5.4 CAVITATION PHOTOGRAPHS d/D = 0,43

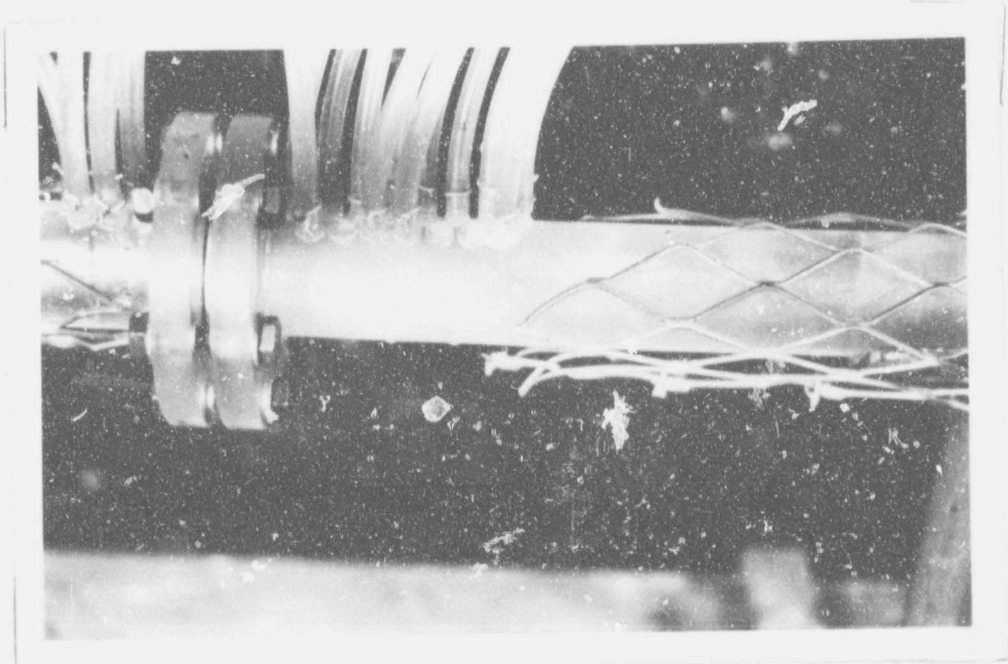

PHOTOGRAPH 3

P_U = 335 kPa ΔP = 290 kPa

Q = 2,66 l/s σ_i = 0,44

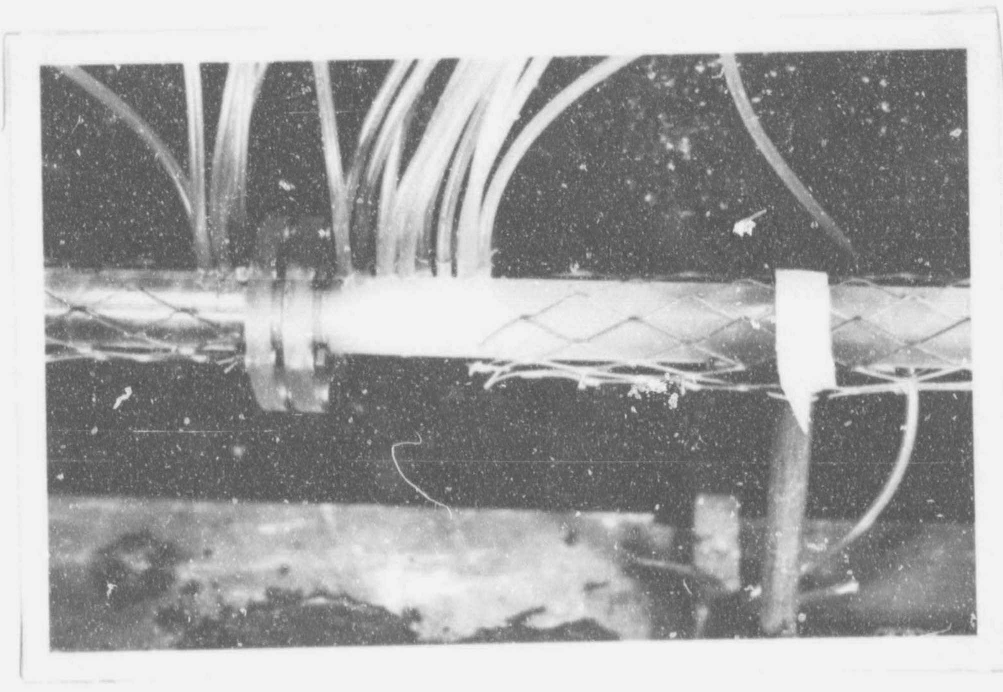

PHOTOGRAPH 4

P_U = 335 kPa ΔP = 312 kPa

Q = 2,7 l/s σ_i = 0,34

FIGURE 5.5 CAVITATION PHOTOGRAPHS d/D = 0,43

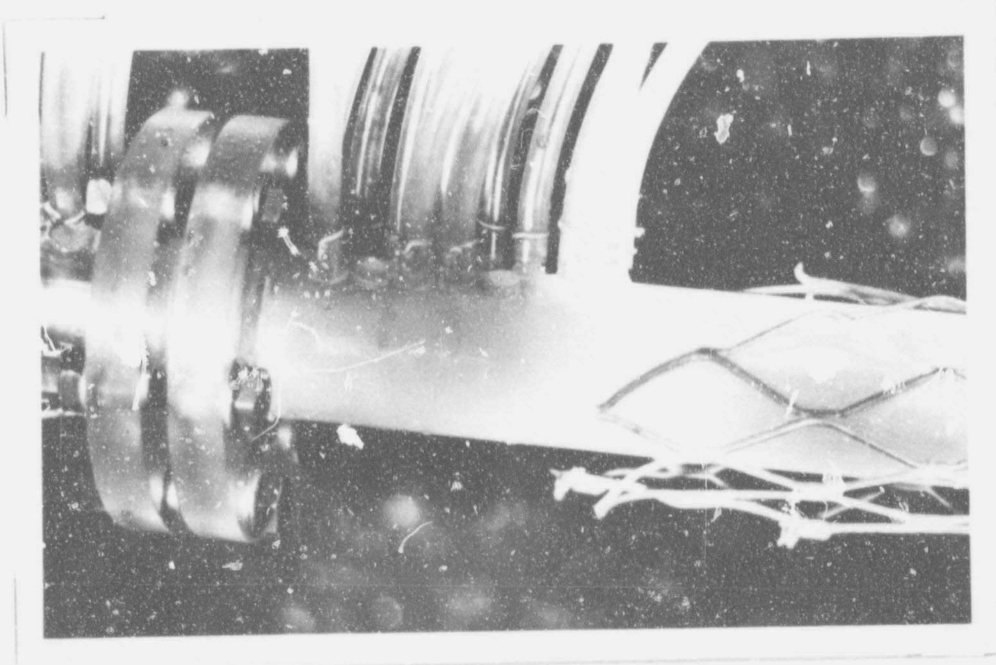

PHOTOGRAPH 5

P_U = 335 kPa ΔP = 320 kPa

Q = 2,74 l/s σ_i = 0,34

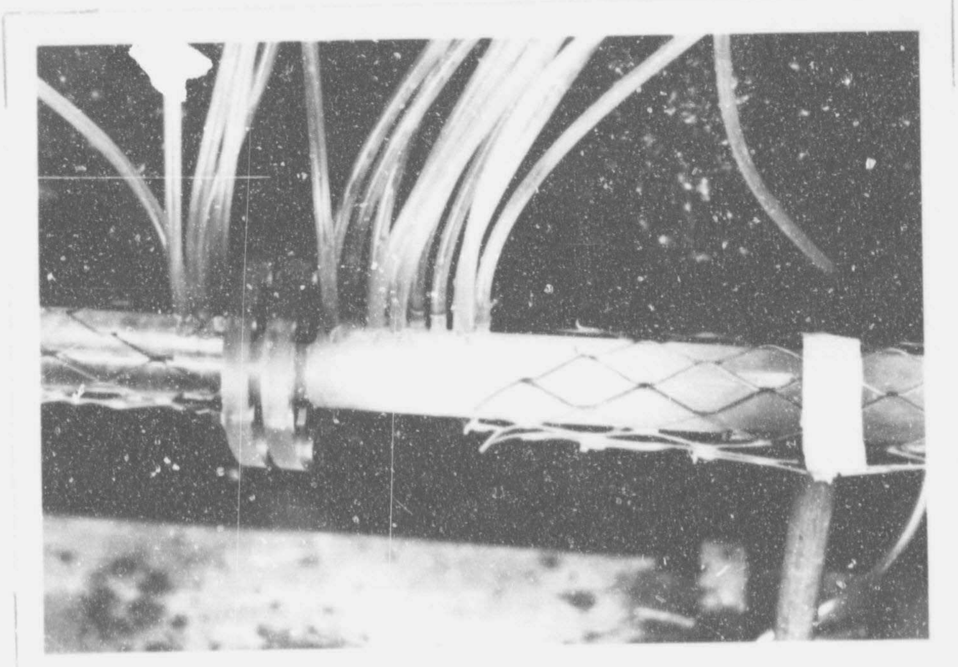

PHOTOGRAPH 6

P_U = 335 kPa ΔP = 325 kPa

Q = 2,8 l/s σ_i = 0,32

FIGURE 5.6 CAVITATION PHOTOGRAPHS d/D = 0,43

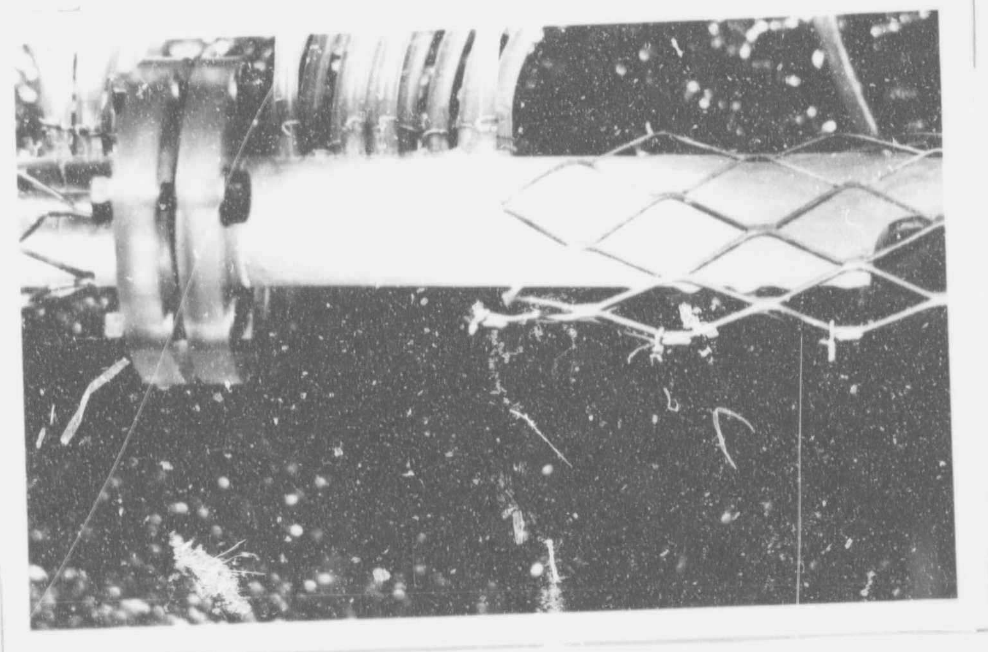

PHOTOGRAPH 7

P_U = 332 kPa ΔP = 327 kPa

Q = [illegible],9 l/s σ_i = 0,28

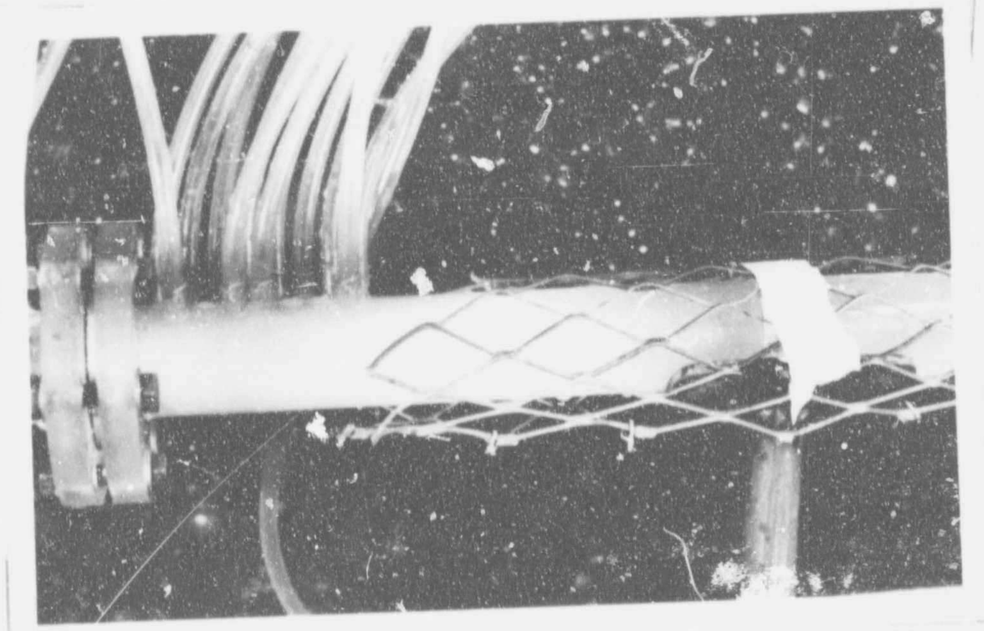

PHOTOGRAPH 8

P_U = 335 kPa ΔP = 330 kPa

Q = 2,82 l/s σ_i = 0,28

FIGURE 5.7 CAVITATION PHOTOGRAPHS d/D = 0,43

However, the area covered by the bubbles at the pipe wall contact area has increased in size, and again the flow region downstream appears aerated. In Figure 5.6 (maximum possible flow) the contact area is at its greatest, and it is impossible to distinguish between the jet and the recirculation zone.

As the contact area represents the area which is exposed to the collapsing cavitation bubbles, the photographs show that a larger area will be exposed to cavitation erosion as flow rates increase. This is substantiated by the work of Ball J.W. et al (1975), where it was found that the area of cavitation erosion downstream of an orifice increased in size longitudinally as the flowrate increased.

In the photographs for the d/D = 0,61 orifice in Figures 5.8 to 5.10, the development of cavitation with flowrate is similarly shown. The onset of cavitation is shown in Figure 5.8, and is again characterised by the cavitation bubbles in the outer layer of jet being just visible. As the flow rate increases the quantity of cavitation bubbles again increases (Figure 5.9), although the jet and recirculation zone are not separately visible. When the flow reached a certain level, 5,5 l/s (Figure 5.9), the visual appearance of cavitation immediately downstream of the orifice changed. In place of cavitation bubbles a jet appearing to contain bubbles and water was visible, while surrounding this was a region of sub-atmospheric pressure, the lowest recorded pressure being - 0,79 bar. The recirculation zone is now visible as a void; however, no recirculation of water was observed. It is significant also that the area for cavitation impingement, or potential damage area, has moved in position to a point further downstram. The effect of this is not known from the erosion aspect, but it does tend to suggest that it may be possible for eros[illegible] mbatted by the introduction of by-passed water, [illegible] ary fluid, into the evacuated area. Where the je[illegible] ts the pipe wall, the area of contact (cavitation bubbles and water) increases in size, coupled with increasing flow and cavitation, as shown in Figures 5.8 and 5.9. In Figure 5.10 the photograph shows that the contact area has further increased in size.

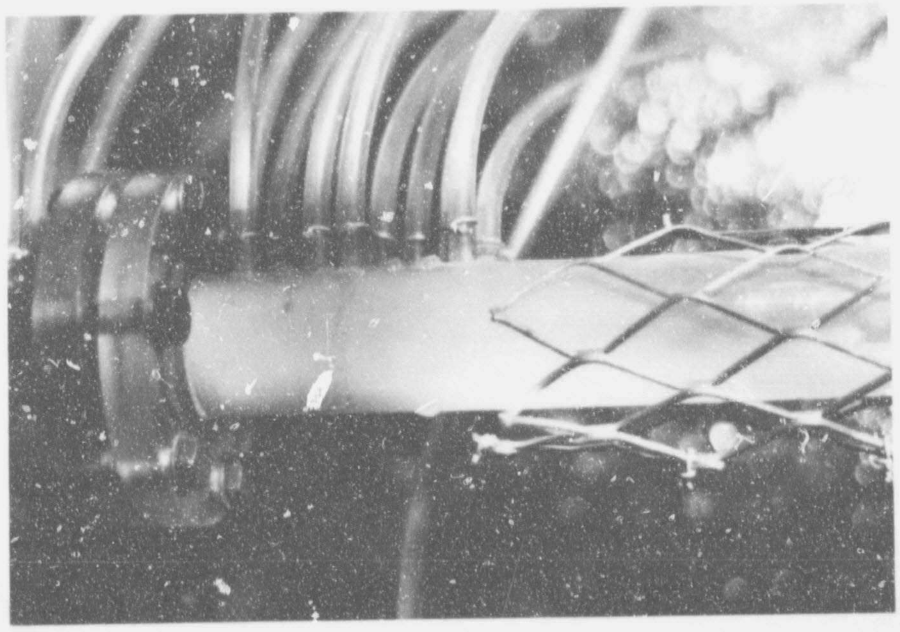

PHOTOGRAPH 9 P_U = 260 kPa ΔP = 234 kPa

Q = 5,17 l/s σ_1 = 0,47

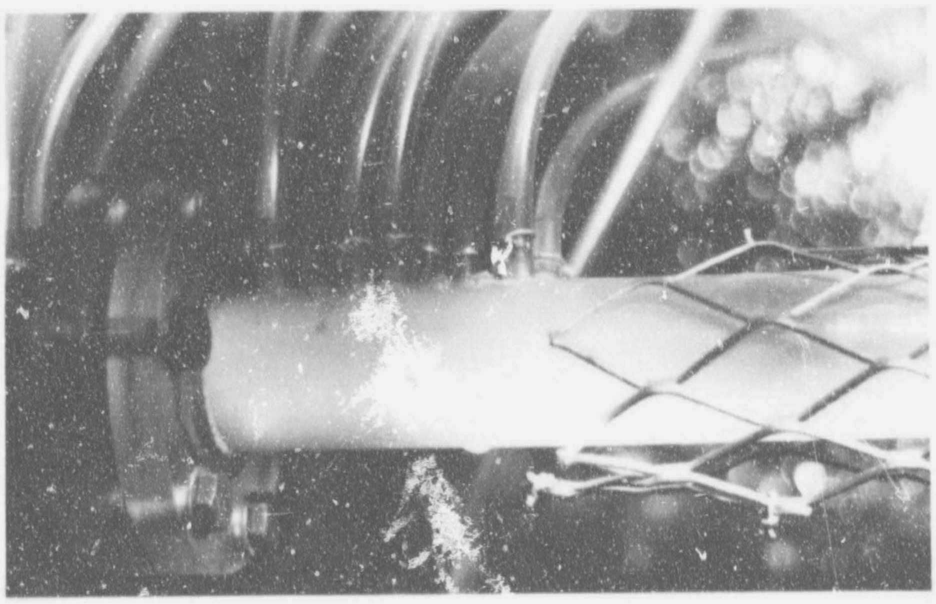

PHOTOGRAPH 10 P_U = 250 kPa ΔP = 225 kPa

Q = 5,46 l/s σ_1 = 0,48

FIGURE 5.8 CAVITATION PHOTOGRAPHS d/D = 0.61

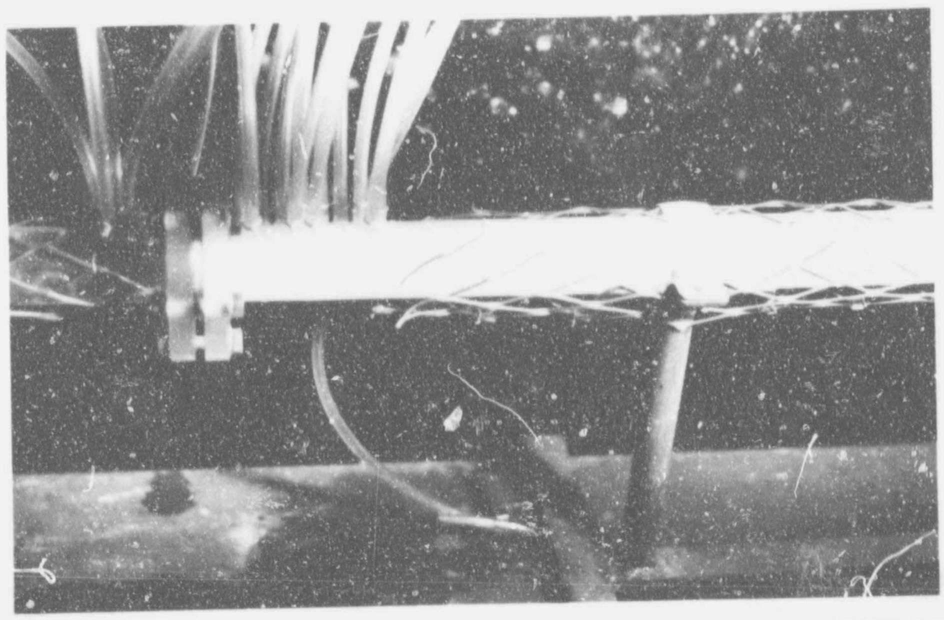

PHOTOGRAPH 11 — P_U = 245 kPa, Q = 5,38 l/s, ΔP = 221 kPa, σ_1 = 0,48

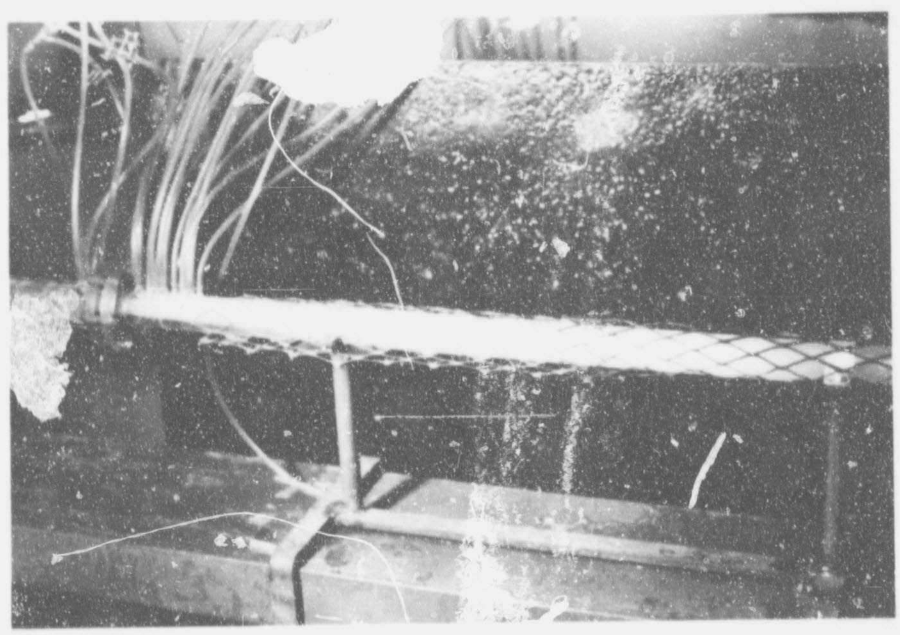

PHOTOGRAPH 12 — P_U = 245 kPa, Q = 5,5 l/s, ΔP = 222 kPa, σ_1 = 0,48

<u>FIGURE 5.9 CAVITATION PHOTOGRAPHS d/D = 0,61</u>

PHOTOGRAPH 13

P_U = 240 kPa
Q = 5,49 l/s

ΔP = 217 kPa
σ_i = 0,49

FIGURE 5.10 CAVITATION PHOTOGRAPHS d/D = 0,61

With regard to the sequence of photographs in Figures 5.9 and 5.10 showing flow through the orifice becoming a distinct jet, this is believed to be due to the rate of cavitation bubble production; that is, the number of bubbles produced, and their expansion downstream of the orifice, is of such a magnitude that they combine and form a vapour pocket in the low pressure area. A further possible reason is that of the vapour pressure is attained immediately downstream of the orifice. However, at 16 °C the vapour pressure is 1,4 kPa (abs), which is below any of the pressures measured downstream of the orifice, hence there would have to be a water temperature increase of approximately 20 °C to achieve a matching of the orifice downstream pressure and the vapour pressure.

When viewed using a stroboscope, the bubbles appeared non-spherical. This can be explained by the fact that with turbulence, the velocities are randomly directed within the flow on a microscopic scale, thus the velocity and pressure gradients cause a bubble to change shape as it passes through a turbulence region.

The area immediately downstream of the orifice consists of a recirculation zone (Figure 5.5) where fast moving fluid on the circumference of the jet is retarded by the fluid outside it, causing it to break away and recirculate back to the orifice. (Cavitation bubbles on the periphery of the jet therefore become detached, and travel back towards the orifice, collapsing near the pipe wall and possibly causing damage to it). The area which is liable for cavitation erosion is thus extended.

On the completion of tests, the downstream perspex pipe was examined for any erosion that might have occurred. The internal pipe surface appeared smooth and undamaged; however, the pressure taps had become pitted internally.

From the test conducted using the vacuum flask, and the samples of disturbed and undisturbed water, the general conclusion that can be drawn is that if water is agitated prior to use in a system, its cavitation resistance is reduced. This supports the work referred to in Section 2.2.1, and is thus an effect liable to make a system more susceptible to cavitation.

Generally, from the test work conducted at the University of the Witwatersrand the general conclusions that can be reached are that cavitation limits require better definition, and that the cavitation prediction equations (Ball J.W. et al 1975) have not been conclusively validated. However, the cavitation photographs well illustrate the way in which an orifice initiates cavitation, while the stroboscope showed the cavitation bubbles to be non-spherical, thus tending to invalidate spherical bubble theories for cavitation to a greater or lesser extent.

5.2 EAST DRIEFONTEIN GOLD MINE

The results of the East Driefontein experiments are given in the Appendix; the pressure drop/flow measurements are displayed in Figure 5.24 along with the theoretical curves. To interpret the cavitation results, cavitation curves were drawn for each orifice size and the respective upstream pressures, one of the curves being shown in Figure 5.11. In place of the cavitation index (Figure 4.5a), the measured pressure drop was used as the horizontal axis; this was done to give a better understanding of the characteristic curve, and to use one measurement only (pressure drop) so reducing potential errors. The incipient cavitation points for each operating condition were determined using the method outlined in Section 4.1.2 (and as applied to the University of the Witwatersrand results discussed in Section 5.1). These results are listed in Table 5.4 alongside the predicted results (Ball J.W. et al, 1975) and recorded aural observations of incipient cavitation. Unfortunately, due to the nature of

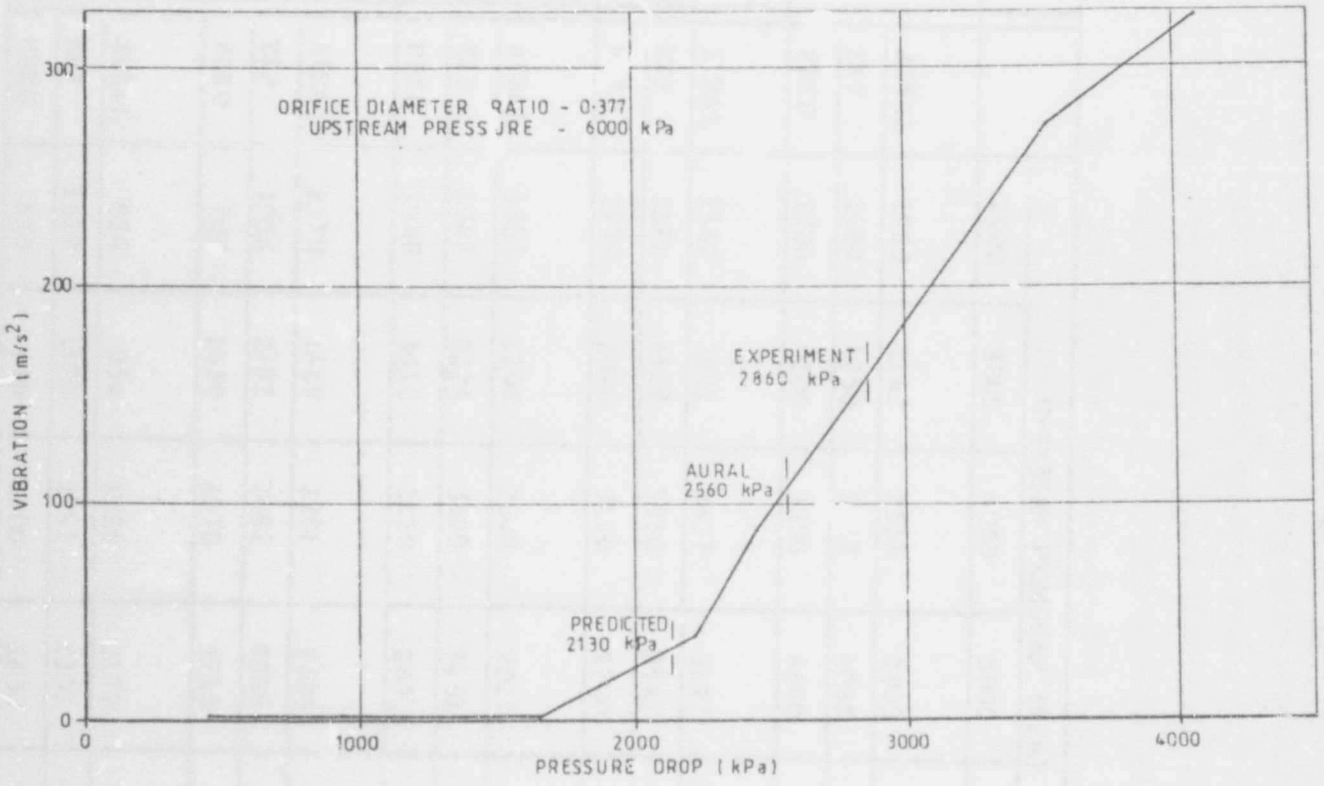

FIGURE 5.11 CAVITATION CURVE - EAST DRIEFONTEIN GOLD MINE

the equipment used underground, it was not possible to take photographs of the cavitation. However, the link between aural and visual tests noted in the University of the Witwatersrand experiments were of value in interpreting the solely aural observations.

d/D		UPSTREAM PRESSURE (kPa) 2000	3000	4000	5000	6000	7000
0,206	AURAL	1985	2143	2559	2903	3633	4673
	EXP	1609	2850	3317	4065	4711	5569
	PRED	2700	4000	5300	6600	8000	9200
0,276	AURAL	1362	1921	2637	3197	3727	4257
	EXP	1377	2429	3050	3542	4134	4668
	PRED	1570	2300	3100	3700	4500	5200
0,330	AURAL	1311	1706	2308	2867	3526	4136
	EXP	1147	2226	3109	3491	3975	4555
	PRED	1010	1610	2120	2650	3200	3700
0,377	AURAL	1170	1669	2201	2024	2560	3415
	EXP	1013	1792	2462	2308	2680	3914
	PRED	700	1050	1370	1710	2130	2400
0,444	AURAL	824	954	1026	2172	2243	-
	EXP	1619	1390	1862	2205	3351	-
	PRED	670	980	1300	1650	1980	-

TABLE 5.4 INCIPIENT CAVITATION PRESSURE DROPS (kPa) FOR EAST DRIEFONTEIN GOLD MINE EXPERIMENTS

For the cavitation curves with the high upstream pressure condition the incipient point was easily determined. However, with some of the low upstream pressure conditions the cavitation curve appeared distorted, and it did not give as clear a picture as did the high upstream pressure tests. This occurred due to the pressure drop and flow through the pressure control valves and vortex flowmeter, the pressure drop and flow generating cavitation external to the orifice. Thus, as the accelerometer, amplifier and RMS voltmeter combination measured total vibration, the resulting cavitation curve was distorted.

5.2.1 OBSERVATIONS

The observations made during the orifice pressure drop tests were as follows:

i) Slight perturbatior [illegible] ontrolled upstream pressure caused rapi [illegible] s in the overall noise level of the system.

ii) On inspection of the test section when orifice plates were changed, it was observed that a small amount of cavitation erosion damage had occurred to the lower section of the pipe wall immediately downstream of the orifice. This was first noticed after approximately 16 hours of operation. The upper section of the pipe appeared undamaged.

iii) Due to the sustained vibration resulting from cavitation, the front support bearing of the test specimen carrier fractured due to fatigue. This was observed at the completion of a test condition, and necessitated seal and specimen carrier replacement.

iv) When sub-atmospheric pressures were attained downstream of the orifice, the resultant vibration and noise was excessive.

5.2.2 ERROR ANALYSIS

Flowrate :

The flowrate was measured primarily by two methods. The first method made use of a vortex flowmeter which was connected to the instrument panel. The second method used orifice plates which were calibrated using the vortex flow meter.

The accuracy of the vortex flowmeter measurements is the sum of the meter accuracy ($\pm$ 2% of flowrate) and the digital display $\pm$ 1 digit ($\pm$ 0,1 l/s). These values combine to give an accuracy of

$$Q\ error\ \% = \pm\left((2)^2 + \left(\frac{0,1\ 100}{Q(l/s)}\right)^2\right)^{0,5} \qquad 5.17$$

The first (downstream of vortex flowmeter) orifice plate accuracy is given by the sum of the vortex flowmeter accuracy and the manometer reading error ($\pm$ 2mm).

$$Q\ error\ \% = \pm\left((2)^2 + \left(\frac{0,1\times 100}{Q(l/s)}\right)^2 + \left(\frac{2\times 100}{\Delta P(mm)}\right)^2\right)^{0,5} \qquad 5.18$$

The second orifice (test orifice) accuracy is given by the root mean sqaure deviation for the fitted equation for calibration, plus the measured pressure drop error

$$Q\ error\ \% = \pm\left((\pm RMSD)^2 + (\pm \Delta P\%)^2\right)^{0,5} \qquad 5.19$$

as given in the following tables -

Q (l/s)	VORTEX FLOW METER (± %)	1st ORIFICE FLOW METER (± %)
20	2,1	10,2
30	2	4,8
40	2	3,2
60	2	2,3
80	2	2,1

d/D	2nd ORIFICE FLOW METER	
	@ 1000 kPa	@ 6000 kPa
0,206	-	-
0,276	3,9	2,9
0,330	4,7	4,0
0,337	11,0	10,7
0,444	9,1	8,7

Pressure measurement

The pressures were measured using a Kistler pressure transducer (0 - 10 MPa, Type No 4043A, Sl No 92737), coupled to a Kistler amplifier (Type 4601, Sl No 23766). The output from the amplifier was given as a digital display on the instrument panel. The accuracy of measurement is given by the transducer error (± 0,5 % of FSD) plus the display error (± 10 kPa):

$$P \text{ error } \% = \pm \left(\left(\frac{50 \times 100}{P(kPa)} \right)^2 + \left(\frac{10 \times 100}{P(kPa)} \right)^2 \right)^{0,5} \qquad 5.20$$

P (kPa)	± % Error
1000	5,1
2000	2,5
3000	1,7
4000	1,3
5000	1
6000	0,85
7000	0,73
8000	0,63
9000	0,57
10 000	0,5

Differential Pressure Measurement :

The differential pressure across the orifice was measured using a differential pressure transmitter (Gould, Mod No. PDH 3000, Sl No. 36337) connected to the digital display of the instrument panel (the ± 1 digit accuracy corresponding to 19,5 kPa). The accuracy of the D.P. transmitter is ± 0,25% of calibrated span (16,3) kPa), calibration being performed by means of the Kistler pressure transducer (± 0,75% at 6530 kPa):

$$\Delta P \text{ error } \% = \left(\left(\frac{16.3 \times 100}{\Delta P(kPa)} \right)^2 + \left(\frac{19.5 \times 100}{\Delta P(kPa)} \right)^2 + (0,75)^2 \right)^{0,5} \qquad 5.21$$

ΔP (kPa)	± % Error
1000	2,7
2000	1,5
3000	1,2
4000	1
5000	0,9
6000	0,9

Vibration :

The vibration set up by the cavitation was measured using an accelerometer (Kistler, type 808A, Sr No. 124821) coupled to a charge amplifier (Kistler, type 504A).

As the level of vibration was used to show the relative intensity of cavitation, the accuracy of measurement has not been estimated.

Flow velocity :

The flow velocity (orifice and pipe) were calculated from flowrate and diameter (hence area) measurements (± 0,05 mm). Up to 50 l/s the vortex flow meter was used, and above 50 l/s the orifice plates were used.

$$V \text{ error}\% = \pm\left((\%Q)^2 + (\%A)^2\right)^{0,5} \quad 5.22$$

Q	PIPE FLOW VELOCITY	ORIFICE d/D				
(l/s)	± %	0,206	0,276	0,330	0,377	0,444
20	2,1	2,1	2,1	2,1	2,1	2,1
30	2	2	2	2	2	2
40	2	2	2	2	2	2
50	2	2	2	2	2	2
60	2,3	2,3	2,9	4,0	10,9	9,1
70	2,2	2,2	2,5	3,7	10,9	9,0
80	2,1	2,1	2,5	3,4	10,8	8,9
90	2,1	2,1	2,5	3,4	10,7	8,9
100	2	2	2,5	3,4	10,6	8,8

Cavitation Number σ_i (Incipient Cavitation results):

The cavitation number is calculated as the ratio of downstream pressure minus the vapour pressure to the pressure drop across the orifice:

$$\sigma_i = \frac{P_D - P_V}{P_U - P_V} \quad 5.23$$

Therefore the error is given by

$$\sigma_i \text{ error}\% = \pm\left((\%P_D)^2 + (\%P_V)^2 + (\%P_U)^2 + (\%P_D)^2\right)^{0,5} \quad 5.24$$

Upstream Pressure (kPa)	ORIFICE d/D				
	0,206	0,276	0,330	0,377	0,444
2000	21,6	13,6	9,6	8,7	7,8
3000	8,5	7,6	6,8	5,8	4,9
4000	4,5	4,8	4,9	4,0	3,3
5000	3,5	3,7	3,9	3,0	2,8
6000	2,8	2,7	2,6	2,4	2,3
7000	2,7	2,8	1,6	1,9	-

<u>Cavitation Number σ_2 (Incipient Cavitation results):</u>

The cavitation number is calculated from the ratio of the downstream pressure minus the vapour pressure, to the velocity head.

$$\sigma_2 = \frac{P_D - P_V}{\rho V^2} \qquad 5.25$$

Therefore the error is given by

$$\sigma_2 \text{ error } \% = \pm\left((\%P_D)^2 + (\%P_V)^2 + 2(\%V)^2\right)^{0,5} \qquad 5.26$$

Upstream Pressure (kPa)	ORIFICE d/D				
	0,206	0,276	0,330	0,377	0,444
2000	15,7	10,1	10,	6,7	6,4
3000	6,8	6,2	5,7	5,1	4,7
4000	4,5	4,6	4,5	4,1	3,8
5000	3,9	3,9	4,1	3,6	3,5
6000	3,6	3,5	3,4	3,4	3,3
7000	3,5	3,5	3,3	3,2	-